Inorg. Chem. **1993,** *32,* 687–694

Unusual Isomers of Edge-Sharing Bioctahedral Complexes

F. A. Cotton,[*] Judith L. Eglin,[†] and Chris A. James[‡]

Department of Chemistry and Laboratory for Molecular Structure and Bonding, Texas A&M University, College Station, Texas 77843

Received August 12, 1992

The edge-sharing bioctahedral complexes 1,2,5,6-$W_2Cl_6(dmpe)_2$ (**1**), 1,2,5,6-$MoWCl_6(dmpe)_2$ (**2**), 1,3,5,7-$MoWCl_6(dmpe)_2$ (**3**), 1,2,5,8-$MoWCl_6$(TETRAPHOS-1) (**4**), and 1,3,5,7-$W_2Cl_6(dmpe)_2$ (**5**) are formed as the oxidative addition products of reactions between the corresponding quadruply bonded complexes and $PhICl_2$ or CH_2Cl_2. Complexes **1**, **2**, and **4** represent new isomeric forms for the $MM'X_6P_4$ core. Complex **4** cocrystallizes with small amounts of 1,2,5,8-Mo_2Cl_6(TETRAPHOS-1) to form a solid solution. The apparent Mo-W distance is 2.718(2) Å for 1,2,5,8-$MoWCl_6$(TETRAPHOS-1). Complexes **2** and **3** are free from contamination by their dimolybdenum analogs and the Mo–W distances are 2.695(1) Å for 1,2,5,6-$MoWCl_6(dmpe)_2$ and 2.7028(5) Å for 1,3,5,7-$MoWCl_6(dmpe)_2$. Complex **1** is isostructural with complex **2** and has a W–W distance of 2.6726(8) Å. The crystal structures of **1**–**4** are fully described. Crystallographic data for these compounds are as follows: Compound **1**, *Pbca* with $a = 13.417(3)$ Å, $b = 14.629(4)$ Å, $c = 13.111(3)$ Å, $V = 2573(1)$ Å^3, and $Z = 4$; compound **2**, *Pbca* with $a = 13.517(5)$ Å, $b = 14.615(5)$ Å, $c = 13.124(4)$ Å, $V = 2593(1)$ Å^3, and $Z = 4$; compound **3**, $P2_1/n$ with $a = 9.2905(1)$ Å, $b = 13.106(2)$ Å, $c = 10.495(2)$ Å, $\beta = 96.13(1)°$, $V = 1270.7(3)$ Å^3, and $Z = 2$; compound **4** $I23$ with $a = b = c = 25.36[2]$ Å, $V = 16322(15)$ Å^3, and $Z = 12$.

Introduction

Edge-sharing bioctahedral (ESBO) complexes constitute an important class of complexes containing multiple metal–metal bonds.[1] There are two synthetic strategies which produce ESBO type complexes, and these in general involve either the formation of a dinuclear unit from two mononuclear units or the oxidative addition of X_2 to a quadruply bonded dinuclear complex.[2-7] Obviously, only the latter of these methodologies would produce heteronuclear ESBO complexes in sufficient purity for further study. However, both of these strategies have been utilized extensively in the Mo_2 and W_2 systems to produce a variety of ESBO complexes.

Only nine distinct geometric isomers for ESBO complexes with a $MM'X_6P_4$ core (where X = Cl, Br, or I and P_4 may be provided by uni- or polydentate phosphines) are possible, as shown in Figure 1. Figure 1 also shows a numbering scheme we shall use to designate the different isomers. Of the complexes that have been reported in the literature, most belong to only the three distinct structural types, *1*, *2*, and *3*. Two completely unprecedented types have now been structurally characterized, one of which has bidentate phosphine ligands and the other a tetradentate phosphine ligand.

Experimental Section

General Procedures. All manipulations were carried out under an atmosphere of argon unless otherwise specified. Standard Schlenk and vacuum line techniques were used. Commercial grade solvents, except alcohols and dichloro- or dibromomethane, were dried over and freshly distilled from potassium/sodium benzophenone ketyl prior to use. Alcohols and dichloro- or dibromomethane were dried over magnesium alkoxides and phosphorus pentoxide respectively and freshly distilled prior to use. α-$W\overset{4}{-}WCl_4(dmpe)_2$,[8] α-$Mo\overset{4}{-}WCl_4(dmpe)_2$,[9] and $Mo\overset{4}{-}WCl_4$(TETRAPHOS-1)[10] were prepared by published procedures. $Mo\overset{4}{-}WCl_4(PMePh_2)_4$ was prepared and purified by the literature method involving the reaction of $Mo(\eta^6\text{-}C_6H_5PMePh)(PMePh_2)_3$ with $WCl_4(PPh_3)_2$ in benzene.[11] Phosphines were purchased from Strem Chemicals and the solids dried in vacuum prior to use. The 1 M $NaBEt_3H$ was purchased from Aldrich and used as received.

The $^{31}P\{^1H\}$ NMR (81-MHz) and ^1H NMR (200-MHz) spectra were recorded on a Varian XL-200 spectrometer. The $^{31}P\{^1H\}$ NMR chemical shift values were referenced externally and are reported relative to 85% H_3PO_4. The IR and UV–visible spectra were recorded on Perkin-Elmer 783 and Cary 17D spectrophotometers, respectively. The rules for naming the different isomers of edge-sharing bioctahedral complexes are discussed in the Results and Discussion section.

Preparation of 1,2,5,6-$W_2Cl_6(dmpe)_2$ (1) and 1,3,5,7-$W_2Cl_6(dmpe)_2$ (5). Method 1. A 0.20-g sample of α-$W\overset{4}{-}WCl_4(dmpe)_2$ was dissolved in 20 mL of CH_2Cl_2 and stirred for 24 h. The initial green color of the solution quickly faded, and it began to turn brown after 1 h. The reaction mixture was allowed to stir for an additional 24 h to ensure completion of the reaction, resulting in a brown solution. The $^{31}P\{^1H\}$ NMR spectrum of this solution indicated that only the edge-sharing complex 1,3,5,7-$W_2Cl_6(dmpe)_2$ was present in more than 60% yield based on integrated intensities of the $^{31}P\{^1H\}$ NMR spectra at low temperatures. However, subsequent evaporation of the solvent under argon produced crystalline 1,2,5,6-$W_2Cl_6(dmpe)_2$ as identified by X-ray diffraction. Only one type of crystals, yellow-brown block shaped, were observed along with a small amount of brown oily precipitate. No attempts were made to optimize the yields in this reaction.

Preparation of 1,2,5,6-$W_2Cl_6(dmpe)_2$ (1). Method 2. A 0.10 g sample (0.307 mmol) of WCl_4 was suspended in 10 mL of THF and 300 μL of $NaBEt_3H$ added to reduce the W(IV) to W(III). The reaction mixture was allowed to stir for 20 min and a solution of dmpe (0.614 mmol) in hexanes added. After the mixture was stirred for 24 h to ensure completion of the reaction, the resulting solution was clear with a large quantity of black precipitate. To this solution 10 mL of CH_2Cl_2 was added and the solution gently heated for 6 h. The red/orange solution was then filtered and 20 mL of hexanes added to produce 0.018 g (7%) of microcrystalline 1,2,5,6-$W_2Cl_6(dmpe)_2$ as identified by $^{31}P\{^1H\}$ NMR spectroscopy.

Preparation of 1,2,5,6-$MoWCl_6(dmpe)_2$ (2). $Mo\overset{4}{-}WCl_4(PMePh_2)_4$ (0.050 g, 0.041 mmol) was dissolved in 10 mL of benzene in a

---

[†] Present address: Mississippi State University, Mississippi State, MS 39762.

[‡] Present address: Los Alamos National Laboratory, INC-14 Los Alamos, NM 87545.

(1) Cotton, F. A. *Polyhedron* **1987**, *6*, 667.

(2) Jackson, R. B.; Streib, W. E. *Inorg. Chem.* **1971**, *10*, 1760.

(3) Schrock, R. R.; Sharp, P. R. *J. Am. Chem. Soc.* **1983**, *102*, 1430.

(4) Canich, J. M.; Cotton, F. A.; Daniels, L. M.; Lewis, D. B. *Inorg. Chem.* **1987**, *26*, 4046.

(5) Chakravarty, A. R.; Cotton, F. A.; Diebold, M. P.; Lewis, D. B.; Roth, W. J. *J. Am. Chem. Soc.* **1986**, *108*, 971.

(6) Agaskar, P. A.; Cotton, F. A.; Dunbar, K. R.; Falvello, L. R.; O'Connor, C. J. *Inorg. Chem.* **1987**, *26*, 4051.

(7) Chacon, S. T.; Chisholm, M. H.; Streib, W. E.; Van Der Sluys, W. *Inorg. Chem.* **1989**, *28*, 5.

(8) Fanwick, P. E.; Harwood, W. S.; Walton, R. A. *Inorg. Chem.* **1987**, *26*, 242.

(9) Cotton, F. A.; James, C. A. Submitted for publication in *Inorg. Chem.*

(10) James, C. A. Ph.D. Dissertation, Texas A&M University, 1992.

(11) Luck, R. L.; Morris, R. H.; Sawyer, J. F. *Inorg. Chem.* **1987**, *26*, 2422.

0020-1669/93/1332-0687$04.00/0

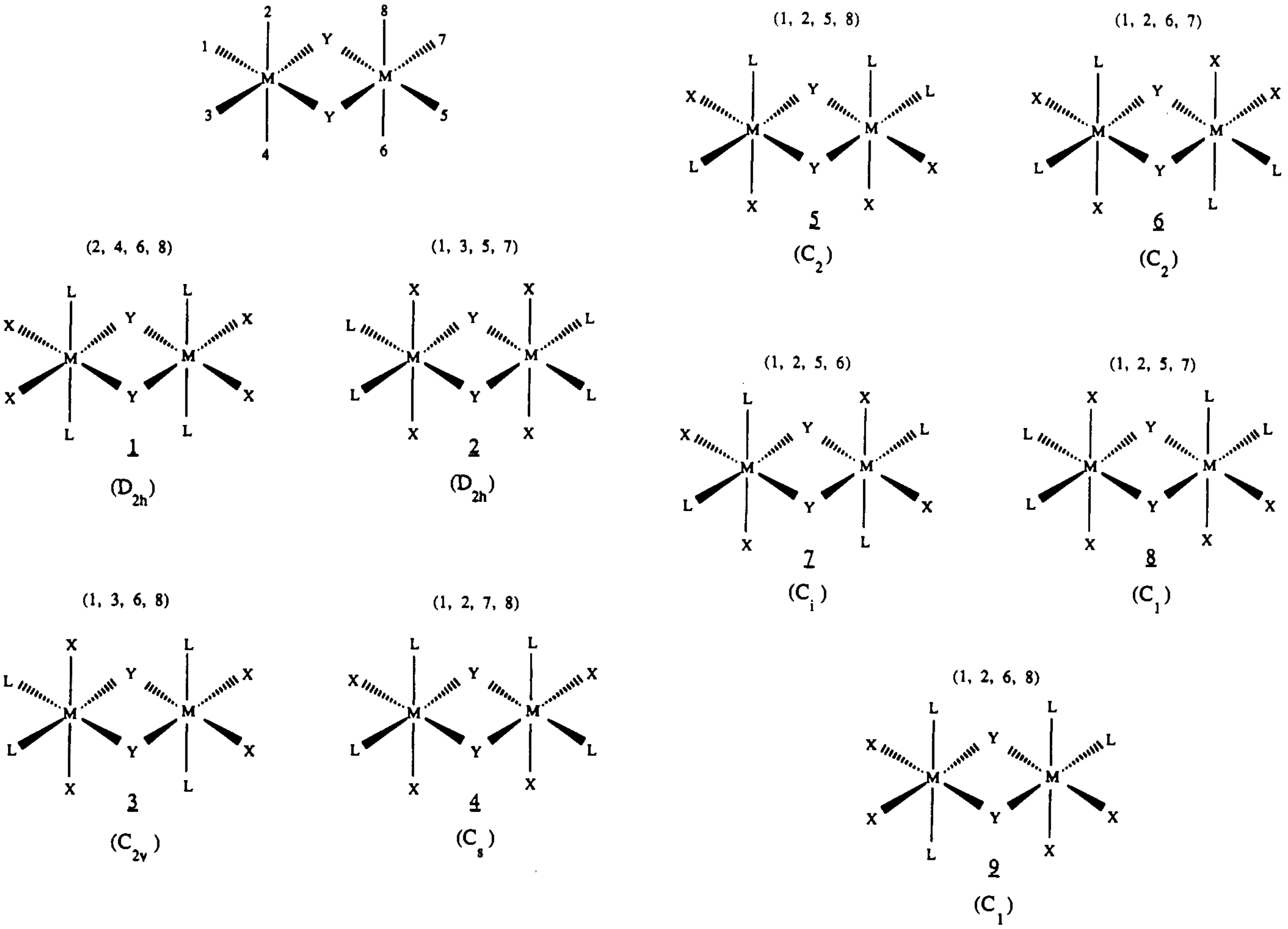

Figure 1. The nine possible isomers for the $M_2(\mu\text{-}X)_2X_4P_4$ core and the numbering system employed to distinguish the isomers.

Schlenk tube. A mixture of benzene and hexanes (1:2) was then layered above this solution. Finally, a solution of dmpe (0.052 g, 0.348 mmol) in 20 mL of hexanes was layered over the benzene/hexanes solvent mixture. This layered mixture was left undisturbed for 1 week, producing 0.010 g (31%) of crystalline 1,2,5,6-MoWCl$_6$(dmpe)$_2$.

Preparation of 1,3,5,7-MoWCl$_6$(dmpe)$_2$ (3). Method 1. Mo$\overset{4}{-}$WCl$_4$(PMePh$_2$)$_4$ (0.050 g, 0.041 mmol) and dmpe (0.025 g, 0.164 mmol) were dissolved in 20 mL of benzene. The reaction mixture was stirred and heated gently for 2 h. Upon heating, the initial green color quickly turned to red-brown. After 2 h the reaction was allowed to cool, and the red product precipitated with hexanes. The precipitate was then filtered, washed with hexanes, and dried in vacuum (0.023 g, 76%).

Preparation of 1,3,5,7-MoWCl$_6$(dmpe)$_2$ (3). Method 2. A 0.025-g sample of α-Mo$\overset{4}{-}$WCl$_4$(dmpe)$_2$ was dissolved in 20 mL of CH$_2$Cl$_2$ and stirred for 24 h. The initial blue-violet color of the solution quickly faded, and it began to turn red-brown after 2 h. The reaction mixture was allowed to stir for an additional 22 h to ensure completion of the reaction, resulting in a red-brown solution. The solvent was allowed to evaporate slowly under argon, producing 0.024 g (86%) of crystalline 1,3,5,7-MoWCl$_6$(dmpe)$_2$ as identified by X-ray diffraction.

Preparation of 1,2,5,8-MoWCl$_6$(TETRAPHOS-1) (4). Method 1. A 0.050-g sample of Mo$\overset{4}{-}$WCl$_4$(TETRAPHOS-1) was dissolved in 15 mL of THF and 0.020 g (0.086 mmol) of PhICl$_2$ added as the chlorinating agent. The solution immediately turned red, and a small amount of red precipitate was produced. The solvent volume was then reduced and 20 mL of hexanes added to afford complete precipitation. The red product (0.048 g, 96%) was then filtered, washed with benzene, and dried in vacuum.

Preparation of 1,2,5,8-MoWCl$_6$(TETRAPHOS-1) (4). Method 2. A 0.050-g sample of Mo$\overset{4}{-}$WCl$_4$(TETRAPHOS-1) was dissolved in 20 mL of CH$_2$Cl$_2$ and stirred for 24 h. The initial green color of the solution slowly faded, and it began to turn red after 4 h. The reaction mixture was allowed to stir for an additional 22 h to ensure completion of the reaction, resulting in a red solution and a small amount of red precipitate. The solution was then filtered into a Schlenk tube and layered with methanol to produce 0.041 g (82%) of microcrystalline 1,2,5,8-MoWCl$_6$(TETRAPHOS-1) as identified by its visible spectrum.

X-ray Crystallography

Single-crystal diffraction experiments were conducted using a Rigaku AFC5 automated diffractometer with Cu Kα radiation for **2** and **3** and an Enraf-Nonius CAD-4S automated diffractometer with Mo Kα radiation for **1** and **4**. Routine unit cell identification and intensity data collection procedures were followed by utilizing the options specified in Tables I and II and the general procedures previously described.[12] Lattice dimensions and Laue symmetry were verified using axial photographs. Three standard reflections were measured every hour during data collections to monitor any gain or loss in intensity, and a correction was applied when ΔI was greater than 3%. Corrections for Lorentz, polarization, and absorption effects were applied to all data sets. The latter correction was based on azimuthal scans of several reflections with diffractometer angle χ near 90°.[13]

General Structure Solution and Refinement. The following general procedures were employed for the solution and refinement of all compounds unless otherwise noted.

The heavy-atom positions were obtained from three-dimensional Patterson functions. The positions for the remainder of the non-hydrogen atoms were found using a series of full matrix refinements followed by difference Fourier syntheses. These positions were initially refined with isotropic thermal parameters and then with anisotropic thermal parameters to convergence. The hydrogen atoms, where included, were placed and fixed at calculated positions and their isotropic thermal parameters constrained to one variable, and the entire model was refined to convergence. For complexes **2–4**, hybrid atoms (MW) composed of 50%

---

(12) Bino, A.; Cotton, F. A.; Fanwick, P. E. *Inorg. Chem.* **1979**, *18*, 3558.

(13) North, A. C. T.; Phillips, D. A.; Matthews, F. S. *Acta Crystallogr., Sect. A: Cryst. Phys., Diffr., Theor. Gen. Crystallogr.* **1968**, *24A*, 351.

Table I. Crystallographic Data and Data Collection Parameters for 1,2,5,6-$W_2Cl_6(dmpe)_2$ (**1**) and 1,2,5,6-$MoWCl_6(dmpe)_2$ (**2**)

	1	**2**
chem formula	$W_2Cl_6P_4C_{12}H_{32}$	$WMoCl_6P_4C_{12}H_{32}$
fw	880.70	792.79
space group (No.)	*Pbca* (61)	*Pbca* (61)
a, Å	13.417(3)	13.517(5)
b, Å	14.629(4)	14.615(5)
c, Å	13.111(3)	13.124(4)
α, deg	(90)	(90)
β, deg	(90)	(90)
γ, deg	(90)	(90)
V, $Å^3$	2573(1)	2593(1)
Z	4	4
T, °C	−80 ± 2	23 ± 2
λ, Å	0.710 73	1.541 84
ρ_{calcd}, g cm^{-3}	2.273	2.031
μ(Mo Kα or Cu Kα), cm^{-1}	100.04	204.85
transm coeff	0.9977–0.3637	1.000–0.7505
R,[a] R_w[b]	0.047, 0.088	0.069, 0.115

[a] $R = \sum||F_o| - |F_c||/\sum|F_o|$. [b] $R_w = [\sum w(|F_o| - |F_c|)^2/\sum w|F_o|^2]^{1/2}$; $w = 1/\sigma^2(|F_o|)$.

Table II. Crystallographic Data and Data Collection Parameters for 1,3,5,7-$MoWCl_6(dmpe)_2$ (**3**) and 1,2,5,8-$MoWCl_6$(TETRAPHOS-1) (**4**)

	3	**4**
chem formula	$WMoCl_6P_4C_{12}H_{32}$	$WMoCl_6P_4C_{42}H_{42}$
fw	792.8	1163.21
space group (No.)	$P2_1/n$ (14)	*I*23 (197)
a, Å	9.2905(1)	25.36[2]
b, Å	13.106(2)	25.36[2]
c, Å	10.495(2)	25.36[2]
α, deg	(90)	(90)
β, deg	96.13(1)	(90)
γ, deg	(90)	(90)
V, $Å^3$	1270.7(3)	16322(15)
Z	2	12
T, °C	23 ± 2	23 ± 2
λ, Å	1.541 84	0.710 73
ρ_{calcd}, g cm^{-3}	2.072	1.893
μ(Mo Kα or Cu Kα), cm^{-1}	208.995	37.62
transm coeff	1.000–0.336	1.000–0.8418
R,[a] R_w[b]	0.0380, 0.0453	0.056, 0.085

[a] $R = \sum||F_o| - |F_c||/\sum|F_o|$. [b] $R_w = [\sum w(|F_o| - |F_c|)^2/\sum w|F_o|^2]^{1/2}$; $w = 1/\sigma^2(|F_o|)$.

Table III. Positional and Thermal Parameters for Non-Hydrogen Atoms of 1,2,5,6-$W_2Cl_6(dmpe)_2$ (**1**)

atom	*x*	*y*	*z*	*B*,[a] $Å^2$
W(1)	0.00619(3)	0.06531(4)	0.07097(4)	1.64(1)
Cl(1)	−0.0473(3)	0.0921(3)	−0.0996(3)	2.39(7)
Cl(2)	0.0382(3)	0.0739(3)	0.2556(3)	2.81(8)
Cl(3)	−0.1713(3)	−0.1306(3)	−0.0404(3)	3.57(9)
P(1)	−0.1703(3)	0.0602(3)	0.1275(3)	2.09(7)
P(2)	−0.0357(3)	0.2325(3)	0.0929(3)	2.37(8)
C(11)	−0.208(1)	−0.034(1)	0.211(1)	3.5(4)
C(12)	−0.193(1)	0.159(1)	0.212(1)	2.7(3)
C(13)	−0.268(1)	0.073(1)	0.031(1)	3.8(4)
C(21)	−0.160(1)	0.245(1)	0.149(1)	3.3(3)
C(22)	0.053(1)	0.294(1)	0.180(1)	4.3(4)
C(23)	−0.044(2)	0.306(1)	−0.018(1)	4.6(4)

[a] Values for anisotropically refined atoms are given in the form of the equivalent isotropic displacement parameter defined as $^1/_3[a^2a^{*2}B_{11} + b^2b^{*2}B_{22} + c^2c^{*2}B_{33} + 2ab(\cos\gamma)a^*b^*B_{12} + 2ac(\cos\beta)a^*c^*B_{13} + 2bc(\cos\alpha)b^*c^*B_{23}]$.

Table IV. Complete Bond Lengths (Å) and Angles (deg) for 1,2,5,6-$W_2Cl_6(dmpe)_2$ (**1**)[a]

	Bond Lengths		
W(1)–W(1)	2.6726(8)	P(1)–C(11)	1.83(2)
W(1)–Cl(1)	2.381(4)	P(1)–C(12)	1.84(2)
W(1)–Cl(1)	2.398(4)	P(1)–C(13)	1.83(2)
W(1)–Cl(2)	2.462(4)	P(2)–C(21)	1.84(2)
W(1)–Cl(3)	2.446(4)	P(2)–C(22)	1.87(2)
W(1)–P(1)	2.482(4)	P(2)–C(23)	1.81(2)
W(1)–P(2)	2.526(4)	C(12)–C(21)	1.57(2)
	Bond Angles		
W(1)–W(1)–Cl(1)	56.3(1)	Cl(3)–W(1)–P(1)	157.7(1)
W(1)–W(1)–Cl(1)	55.69(9)	Cl(3)–W(1)–P(2)	80.9(1)
W(1)–W(1)–Cl(2)	137.1(1)	P(1)–W(1)–P(2)	77.5(1)
W(1)–W(1)–Cl(3)	102.8(1)	W(1)–Cl(1)–W(1)	68.0(1)
W(1)–W(1)–P(1)	97.31(9)	W(1)–P(1)–C(11)	117.7(5)
W(1)–W(1)–P(2)	139.26(9)	W(1)–P(1)–C(12)	108.1(5)
Cl(1)–W(1)–Cl(1)	112.0(1)	W(1)–P(1)–C(13)	118.0(5)
Cl(1)–W(1)–Cl(2)	165.4(1)	C(11)–P(1)–C(12)	100.5(8)
Cl(1)–W(1)–Cl(3)	93.1(1)	C(11)–P(1)–C(13)	107.4(8)
Cl(1)–W(1)–P(1)	89.9(1)	C(12)–P(1)–C(13)	102.7(8)
Cl(1)–W(1)–P(2)	83.1(1)	W(1)–P(2)–C(21)	110.4(6)
Cl(1)–W(1)–Cl(2)	81.7(1)	W(1)–P(2)–C(22)	113.1(6)
Cl(1)–W(1)–Cl(3)	101.1(1)	W(1)–P(2)–C(23)	119.6(6)
Cl(1)–W(1)–P(1)	98.3(1)	C(21)–P(2)–C(22)	106.3(8)
Cl(1)–W(1)–P(2)	164.5(1)	C(21)–P(2)–C(23)	102.2(9)
Cl(2)–W(1)–Cl(3)	89.0(1)	C(22)–P(2)–C(23)	104.0(9)
Cl(2)–W(1)–P(1)	82.8(1)	P(1)–C(12)–C(21)	106.(1)
Cl(2)–W(1)–P(2)	83.0(1)	P(2)–C(21)–C(12)	112.(1)

[a] Numbers in parentheses are estimated standard deviations in the least significant digit.

Mo and 50% W were placed at the metal atom positions in the initial stages of the refinement. Final refinements employed the SHELX-76 package of programs with variations in occupancy factors used to determine the composition of the metal atom sites. Important details pertinent to individual compounds are presented in Tables I and II and in the following paragraphs.

Compound 1. Crystals of 1,2,5,6-$W_2Cl_6(dmpe)_2$ were obtained by the slow evaporation of CH_2Cl_2 from a solution of the complex. Only one type of crystal, block shaped, was observed along with some oily brown residue. A yellow-brown block shaped crystal was selected, coated with fluorocarbon grease, and mounted on the end of a quartz fiber.

Systematic absences uniquely determined the space group as *Pbca*. The difference Fourier map contained large "ghost" peaks in close proximity to the heavy atom positions. The residuals, at convergence with isotropic thermal parameters, were $R = 0.137$ and $R_w = 0.084$. A calculated absorption correction utilizing the DIFABS[14] program was now applied to the data set. After the application of this correction, the model was allowed to refine freely first with isotropic and then with anisotropic thermal parameters to convergence. The final refinement factors after convergence are listed in Table I. Table III contains positional and thermal parameters for non-hydrogen atoms. Complete bond lengths and angles are listed in Table IV, and an ORTEP diagram of the molecule is given in Figure 2. Tables of anisotropic thermal parameters are available as supplementary material.

Compound 2. Crystals of 1,2,5,6-$MoWCl_6(dmpe)_2$ were obtained as described in the Experimental Section. A yellow-brown block shaped crystal was selected, coated with epoxy cement, and mounted on the end of a glass fiber. The standards monitored during data collection indicated that the crystal had decayed 4.5%, and a correction was made for this.

Systematic absences uniquely determined the space group as *Pbca*. The residuals, at convergence with isotropic thermal parameters, were $R = 0.1014$ and $R_w = 0.1236$, but the difference Fourier map contained "ghost" peaks close to the heavy atom positions. A calculated absorption correction utilizing the DIFABS[14] program was therefore applied, and the model was then allowed to refine freely, first with isotropic and then with anisotropic thermal parameters, to convergence. Because both initial and subsequent refinements in the hybrid metal atom composition failed to indicate the presence of 1,2,5,6-$Mo_2Cl_6(dmpe)_2$, the hybrid metal atom composition was fixed at 50.0% Mo and 50.0% W in the final refinement. The final refinement factors after convergence are listed in Table I. Table V contains positional and thermal parameters for non-hydrogen atoms. Complete bond lengths and angles are listed in Table VI and an ORTEP diagram of the molecule is given in Figure 3. Tables of anisotropic thermal parameters are available as supplementary material.

Compound 3. Crystals of 1,3,5,7-$MoWCl_6(dmpe)_2$ were obtained by slow evaporation of CH_2Cl_2 as described in the Experimental Section. A red-black cube shaped crystal was selected, coated with epoxy cement, and mounted on the end of a glass fiber. The standards monitored during data collection indicated the crystal had decayed 4.9%, and the data set was subsequently corrected for the decay.

---

(14) North, A. C. T.; Phillips, D. A.; Matthews, F. S. *Acta Crystallogr.* **1983**, *A39*, 159.

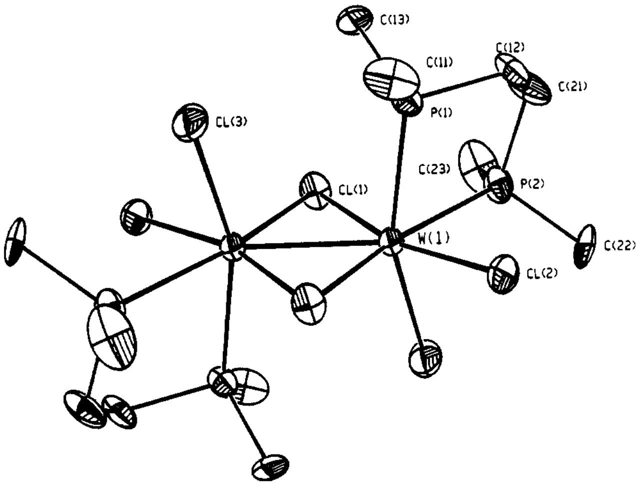

Figure 2. ORTEP drawing of 1,2,5,6-$W_2Cl_6(dmpe)_2$. Thermal ellipsoids are drawn at 50% probability.

Table V. Positional and Thermal Parameters for Non-Hydrogen Atoms of 1,2,5,6-$MoWCl_6(dmpe)_2$ (**2**)

atom	*x*	*y*	*z*	*B*,[a] Å^2
MW(1)[b]	–0.00587(7)	0.06603(7)	0.07141(7)	1.41(2)
Cl(1)	0.0481(4)	0.0921(3)	–0.0986(3)	2.28(8)
Cl(2)	–0.0377(4)	0.0736(4)	0.2549(4)	3.0(1)
Cl(3)	–0.1692(4)	0.1314(4)	0.0395(4)	3.6(1)
P(1)	0.0364(4)	0.2335(3)	0.0944(4)	2.03(9)
P(2)	0.1708(4)	0.0612(3)	0.1288(4)	1.80(8)
C(11)	0.039(2)	0.307(2)	–0.015(2)	4.6(6)
C(12)	0.158(2)	0.248(2)	0.155(2)	3.9(5)
C(13)	–0.048(2)	0.296(2)	0.181(2)	4.4(6)
C(21)	0.189(2)	0.160(1)	0.211(1)	2.6(4)
C(22)	0.206(2)	–0.032(1)	0.211(2)	3.6(4)
C(23)	0.266(1)	0.070(2)	0.036(2)	2.9(4)

[a] Values for anisotropically refined atoms are given in the form of the equivalent isotropic displacement parameter defined as $^1/_3[a^2a^{*2}B_{11} + b^2b^{*2}B_{22} + c^2c^{*2}B_{33} + 2ab(\cos\gamma)a^*b^*B_{12} + 2ac(\cos\beta)a^*c^*B_{13} + 2bc(\cos\alpha)b^*c^*B_{23}]$. [b] Hybrid metal atom composed of 50.0% Mo and 50.0% W.

Systematic absences uniquely determined the space group as $P2_1/n$. The residuals, at convergence with isotropic thermal parameters, were $R = 0.0797$ and $R_w = 0.0945$. A calculated absorption correction utilizing the DIFABS[14] program was then applied, and the model was allowed to refine freely, first with isotropic and then with anisotropic thermal parameters, to convergence. The initial and subsequent refinements of the hybrid metal atom composition failed to indicate the presence of 1,3,5,7-$Mo_2Cl_6(dmpe)_2$. Therefore, the hybrid metal atom composition was fixed at 50.0% Mo and 50.0% W in the final refinement. The final refinement factors after convergence are listed in Table II. Table VII contains positional and thermal parameters for non-hydrogen atoms. Complete bond lengths and angles are listed in Table VIII. An ORTEP diagram of the molecule is given in Figure 3. Tables of anisotropic thermal parameters are available as supplementary material.

Compound 4. Crystals of 1,2,5,8-$MoWCl_6$(TETRAPHOS-1) were obtained by layering a dilute CH_2Cl_2 solution of this compound with a mixture of benzene and methanol (1:2) in a long glass tube sealed under an argon atmosphere. A red needle-shaped crystal was selected from the tube and mounted on the end of a glass fiber with epoxy cement.

The axial photographs failed to indicate the Laue class, and the systematic absences left six possible space groups. However, the expected molecular symmetry eliminated four of these space groups because they were too high in symmetry. This left only $I23$ (No. 197) and $I2_13$ (No. 199). The space group $I23$ was chosen and resulted in satisfactory refinement. Both isomers of the enantiomeric pair were refined, and the isomer reported here gave significantly lower residuals.

The final difference Fourier map showed only one peak above 1 e/Å^3, and this peak was in close proximity to the metal center. The composition of the hybrid metal atom was 55.8 (16)% Mo and 44.2 (16)% W in the final refinement, for which the figures of merit are listed in Table II. Table IX contains positional and thermal parameters for non-hydrogen atoms. Selected bond lengths and angles are listed in Table X. An ORTEP diagram of the molecule is given in Figure 4, and tables of anisotropic thermal parameters, complete bond lengths and angles, and hydrogen atom positional parameters are available as supplementary material.

Table VI. Complete Bond Lengths (Å) and Angles (deg) for 1,2,5,6-$MoWCl_6(dmpe)_2$ (**2**)[a]

Bond Lengths			
MW(1)[b]–MW(1)	2.695(1)	P(1)–C(11)	1.79(2)
MW(1)–Cl(1)	2.378(5)	P(1)–C(12)	1.84(2)
MW(1)–Cl(1)	2.408(5)	P(1)–C(13)	1.85(3)
MW(1)–Cl(2)	2.449(5)	P(2)–C(21)	1.82(2)
MW(1)–Cl(3)	2.442(5)	P(2)–C(22)	1.80(2)
MW(1)–P(1)	2.532(5)	P(2)–C(23)	1.78(2)
MW(1)–P(2)	2.504(5)	C(12)–C(21)	1.54(3)
Bond Angles			
MW(1)–MW(1)–Cl(1)	56.2(1)	Cl(2)–MW(1)–P(2)	82.7(2)
MW(1)–MW(1)–Cl(1)	55.2(1)	Cl(3)–MW(1)–P(1)	81.1(2)
MW(1)–MW(1)–Cl(2)	136.6(1)	Cl(3)–MW(1)–P(2)	157.6(2)
MW(1)–MW(1)–Cl(3)	102.4(1)	P(1)–MW(1)–P(2)	77.1(2)
MW(1)–MW(1)–P(1)	139.6(1)	MW(1)–Cl(1)–MW(1)	68.5(1)
MW(1)–MW(1)–P(2)	97.6(1)	MW(1)–P(1)–C(11)	119.2(8)
Cl(1)–MW(1)–Cl(1)	111.5(2)	MW(1)–P(1)–C(12)	111.2(8)
Cl(1)–MW(1)–Cl(2)	165.8(2)	MW(1)–P(1)–C(13)	114.2(9)
Cl(1)–MW(1)–Cl(3)	93.1(2)	C(11)–P(1)–C(12)	105(1)
Cl(1)–MW(1)–P(1)	83.5(2)	C(11)–P(1)–C(13)	102(1)
Cl(1)–MW(1)–P(2)	89.7(2)	C(12)–P(1)–C(13)	103(1)
Cl(1)–MW(1)–Cl(2)	81.7(2)	MW(1)–P(2)–C(21)	106.7(7)
Cl(1)–MW(1)–Cl(3)	100.8(2)	MW(1)–P(2)–C(22)	117.2(8)
Cl(1)–MW(1)–P(1)	164.6(2)	MW(1)–P(2)–C(23)	118.8(7)
Cl(1)–MW(1)–P(2)	98.9(2)	C(21)–P(2)–C(22)	102(1)
Cl(2)–MW(1)–Cl(3)	89.6(2)	C(21)–P(2)–C(23)	104(1)
Cl(2)–MW(1)–P(1)	83.0(2)	C(22)–P(2)–C(23)	106(1)
P(1)–C(12)–C(21)	111(2)	P(2)–C(21)–C(12)	110(1)

[a] Numbers in parentheses are estimated standard deviations in the least significant digit. [b] Hybrid metal atom composed of 50.0% Mo and 50.0% W.

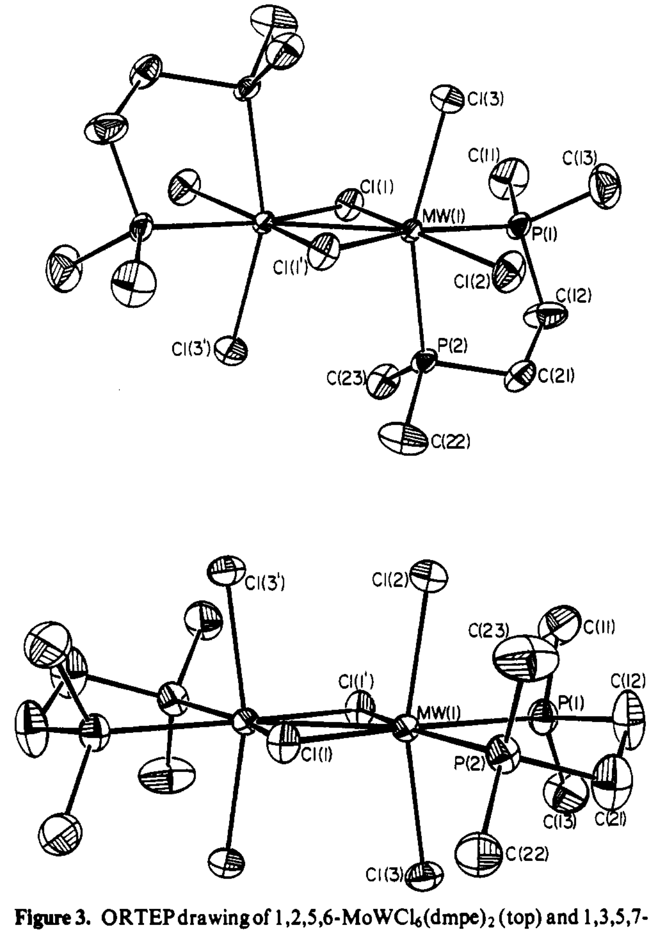

Figure 3. ORTEP drawing of 1,2,5,6-$MoWCl_6(dmpe)_2$ (top) and 1,3,5,7-$MoWCl_6(dmpe)_2$ (bottom). Note the differences in the ligand arrangement for these two different geometries. Thermal ellipsoids are drawn at 50% probability.

Table VII. Positional and Thermal Parameters for Non-Hydrogen Atoms of 1,3,5,7-$MoWCl_6(dmpe)_2$ (3)

atom	*x*	*y*	*z*	*B*,[a] Å^2
MW(1)[b]	0.04283(4)	0.05503(3)	0.10620(3)	1.50(1)
Cl(1)	0.2079(2)	−0.0357(1)	−0.0176(2)	2.19(4)
Cl(2)	0.0324(2)	−0.0780(2)	0.2620(2)	2.63(4)
Cl(3)	0.0759(2)	0.2162(1)	0.0019(2)	2.43(4)
P(1)	−0.0665(2)	0.1597(2)	0.2719(2)	2.25(4)
P(2)	0.2707(2)	0.1107(2)	0.2377(2)	2.16(4)
C(11)	−0.199(1)	0.0954(7)	0.361(1)	4.0(2)
C(13)	−0.160(1)	0.2785(8)	0.2200(9)	4.2(2)
C(12)	0.082(1)	0.1972(9)	0.3934(8)	4.1(2)
C(22)	0.416(1)	0.1620(8)	0.1542(9)	3.8(2)
C(21)	0.217(1)	0.2215(8)	0.3341(9)	4.0(2)
C(23)	0.365(1)	0.0209(9)	0.351(1)	4.8(3)

[a] Values for anisotropically refined atoms are given in the form of the equivalent isotropic displacement parameter defined as $^1/_3[a^2a^{*2}B_{11} + b^2b^{*2}B_{22} + c^2c^{*2}B_{33} + 2ab(\cos\gamma)a^*b^*B_{12} + 2ac(\cos\beta)a^*c^*B_{13} + 2bc(\cos\alpha)b^*c^*B_{23}]$. [b] Hybrid metal atom composed of 50.0% Mo and 50.0% W.

Table VIII. Complete Bond Lengths (Å) and Angles (deg) for 1,3,5,7-$MoWCl_6(dmpe)_2$ (3)[a]

Bond Lengths			
MW(1)[b]–MW(1)	2.7028(5)	P(1)–C(11)	1.83(1)
MW(1)–Cl(1)	2.425(2)	P(1)–C(13)	1.84(1)
MW(1)–Cl(1)	2.428(2)	P(1)–C(12)	1.845(9)
MW(1)–Cl(2)	2.400(2)	P(2)–C(22)	1.81(1)
MW(1)–Cl(3)	2.414(2)	P(2)–C(21)	1.87(1)
MW(1)–P(1)	2.513(2)	P(2)–C(23)	1.83(1)
MW(1)–P(2)	2.509(2)	C(12)–C(21)	1.49(1)
Bond Angles			
MW(1)–MW(1)–Cl(1)	56.20(4)	Cl(3)–MW(1)–P(1)	85.24(6)
MW(1)–MW(1)–Cl(1)	56.11(4)	Cl(3)–MW(1)–P(2)	81.61(6)
MW(1)–MW(1)–Cl(2)	98.31(5)	P(1)–MW(1)–P(2)	80.80(6)
MW(1)–MW(1)–Cl(3)	97.66(4)	MW(1)–Cl(1)–MW(1)	67.69(5)
MW(1)–MW(1)–P(1)	139.20(5)	MW(1)–P(1)–C(11)	116.5(3)
MW(1)–MW(1)–P(2)	139.98(5)	MW(1)–P(1)–C(13)	118.1(3)
Cl(1)–MW(1)–Cl(1)	112.31(6)	MW(1)–P(1)–C(12)	107.2(3)
Cl(1)–MW(1)–Cl(2)	94.75(7)	C(11)–P(1)–C(13)	102.6(5)
Cl(1)–MW(1)–Cl(3)	93.87(6)	C(11)–P(1)–C(12)	105.4(4)
Cl(1)–MW(1)–P(1)	164.58(6)	C(13)–P(1)–C(12)	106.0(5)
Cl(1)–MW(1)–P(2)	83.84(6)	MW(1)–P(2)–C(22)	118.0(3)
Cl(1)–MW(1)–Cl(2)	94.48(7)	MW(1)–P(2)–C(21)	105.4(3)
Cl(1)–MW(1)–Cl(3)	94.64(6)	MW(1)–P(2)–C(23)	119.2(4)
Cl(1)–MW(1)–P(1)	83.09(6)	C(22)–P(2)–C(21)	103.2(5)
Cl(1)–MW(1)–P(2)	163.70(6)	C(22)–P(2)–C(23)	103.0(5)
Cl(2)–MW(1)–Cl(3)	164.03(6)	C(21)–P(2)–C(23)	106.5(5)
Cl(2)–MW(1)–P(1)	82.87(7)	P(1)–C(12)–C(21)	111.6(6)
Cl(2)–MW(1)–P(2)	85.98(6)	P(2)–C(21)–C(12)	110.2(7)

[a] Numbers in parentheses are estimated standard deviations in the least significant digit. [b] Hybrid metal atom composed of 50.0% Mo and 50.0% W.

Results and Discussion

Synthesis. The preparation of complexes **2**–**4** proceeds straightforwardly via oxidative addition of Cl_2, via $PhICl_2$ [phenyldichloroiodine(III)], to the appropriate quadruply bonded species. However, if any of the analogous dimolybdenum complexes are present they are also oxidized, and mixtures of $MoWCl_6(L\text{-}L)_2$ and $Mo_2Cl_6(L\text{-}L)_2$ where L-L = a bidentate phosphine ligand are nearly impossible to separate. A more selective oxidant for the $Mo\overset{4}{-}W$ core is CH_2Cl_2. When solutions of $Mo\overset{4}{-}W$ complexes in CH_2Cl_2 are stirred for several hours at room temperature, the dichloromethane oxidizes only the $Mo\overset{4}{-}WCl_4(L\text{-}L)_2$ complexes to $MoWCl_6(L\text{-}L)_2$ type complexes, leaving the $Mo\overset{4}{-}MoCl_4(L\text{-}L)_2$ complexes unchanged. This selectivity is presumably a result of the difference in the oxidation potentials of the Mo_2, MoW, W_2 triad.[11,15,16]

Table IX. Positional and Thermal Parameters for Non-Hydrogen Atoms of 1,2,5,8-$MoWCl_6$(TETRAPHOS-1) (4)

atom	*x*	*y*	*z*	*B*,[a] Å^2
MW(1)[b]	0.04788(5)	0.52403(5)	0.76919(5)	2.59(3)
Cl(1)	−0.0352(2)	0.5689(2)	0.7684(2)	3.6(1)
Cl(2)	0.0607(2)	0.5232(2)	0.6748(2)	3.5(1)
Cl(3)	0.0879(2)	0.6109(2)	0.7693(3)	3.9(1)
P(1)	0.0607(2)	0.5405(3)	0.8668(2)	3.4(1)
P(2)	0.1429(2)	0.4913(3)	0.7794(2)	3.4(1)
C(11)	0.031(1)	0.498(1)	0.9157(9)	4.2(6)
C(12)	0.131(1)	0.528(1)	0.880(1)	4.4(6)
C(21)	0.1511(9)	0.4811(9)	0.8512(8)	3.4(5)
C(121)	0.0457(6)	0.6034(7)	0.8980(6)	5.0(7)
C(122)	0.0675(6)	0.6121(7)	0.9477(6)	4.9(7)
C(123)	0.0624(6)	0.6613(7)	0.9718(6)	6.3(9)
C(124)	0.0355(6)	0.7018(7)	0.9461(6)	7(1)
C(125)	0.0136(6)	0.6931(7)	0.8964(6)	5.7(8)
C(126)	0.0188(6)	0.6439(7)	0.8723(6)	5.3(7)
C(211)	0.1598(7)	0.4271(7)	0.7511(6)	4.7(7)
C(212)	0.1763(7)	0.3853(7)	0.7828(6)	6.3(9)
C(213)	0.1915(7)	0.3377(7)	0.7599(6)	6.3(9)
C(214)	0.1902(7)	0.3318(7)	0.7052(6)	6.6(9)
C(215)	0.1737(7)	0.3736(7)	0.6735(6)	5.6(8)
C(216)	0.1585(7)	0.4213(7)	0.6964(6)	4.3(7)
C(221)	0.1940(7)	0.5349(8)	0.7583(7)	3.8(6)
C(222)	0.1890(7)	0.5596(8)	0.7094(7)	5.3(8)
C(223)	0.2297(7)	0.5914(8)	0.6904(7)	7(1)
C(224)	0.2753(7)	0.5985(8)	0.7203(7)	9(1)
C(225)	0.2803(7)	0.5738(8)	0.7692(7)	10(1)
C(226)	0.2396(7)	0.5420(8)	0.7882(7)	5.9(8)

[a] Values for anisotropically refined atoms are given in the form of the equivalent isotropic displacement parameter defined as $^1/_3[a^2a^{*2}B_{11} + b^2b^{*2}B_{22} + c^2c^{*2}B_{33} + 2ab(\cos\gamma)a^*b^*B_{12} + 2ac(\cos\beta)a^*c^*B_{13} + 2bc(\cos\alpha)b^*c^*B_{23}]$. [b] Hybrid metal atom composed of 55.8 (16)% Mo and 44.2 (16)% W.

Table X. Selected Bond Lengths (Å) and Angles (deg) for 1,2,5,8-$MoWCl_6$(TETRAPHOS-1) (4)[a]

Bond Lengths			
MW(1)[b]–MW(1)	2.718(2)	P(1)–C(12)	1.85(3)
MW(1)–Cl(1)	2.395(5)	P(1)–C(121)	1.82(2)
MW(1)–Cl(1)	2.379(5)	P(2)–C(21)	1.85(2)
MW(1)–Cl(2)	2.417(5)	P(2)–C(211)	1.83(2)
MW(1)–Cl(3)	2.427(6)	P(2)–C(221)	1.79(2)
MW(1)–P(1)	2.532(6)	C(11)–C(11)	1.56(3)
MW(1)–P(2)	2.562(6)	C(12)–C(21)	1.50(3)
P(1)–C(11)	1.82(2)		
Bond Angles			
MW(1)–MW(1)–Cl(1)	55.0(1)	Cl(2)–MW(1)–P(1)	162.4(2)
MW(1)–MW(1)–Cl(1)	55.6(1)	Cl(2)–MW(1)–P(2)	88.4(2)
MW(1)–MW(1)–Cl(2)	96.6(1)	Cl(3)–MW(1)–P(1)	78.2(2)
MW(1)–MW(1)–Cl(3)	141.4(2)	Cl(3)–MW(1)–P(2)	84.3(2)
MW(1)–MW(1)–P(1)	100.9(1)	P(1)–MW(1)–P(2)	80.4(2)
MW(1)–MW(1)–P(2)	134.0(2)	MW(1)–Cl(1)–MW(1)	69.4(2)
Cl(1)–MW(1)–Cl(1)	110.6(2)	C(11)–P(1)–C(12)	100.(1)
Cl(1)–MW(1)–Cl(2)	96.6(2)	C(11)–P(1)–C(121)	98(1)
Cl(1)–MW(1)–Cl(3)	86.4(2)	C(12)–P(1)–C(121)	105.(1)
Cl(1)–MW(1)–P(1)	92.5(2)	C(21)–P(2)–C(211)	103.5(9)
Cl(1)–MW(1)–P(2)	169.3(2)	C(21)–P(2)–C(221)	107(1)
Cl(1)–MW(1)–Cl(2)	90.0(2)	C(211)–P(2)–C(221)	105.2(9)
Cl(1)–MW(1)–Cl(3)	163.0(2)	P(1)–C(11)–C(11)	112.(2)
Cl(1)–MW(1)–P(1)	100.9(2)	P(1)–C(12)–C(21)	112.(2)
Cl(1)–MW(1)–P(2)	78.9(2)	P(2)–C(21)–C(12)	110.(2)
Cl(2)–MW(1)–Cl(3)	87.3(2)		

[a] Numbers in parentheses are estimated standard deviations in the least significant digit. [b] Hybrid metal atom composed of 55.8 (16)% Mo and 44.2 (16)% W.

α-$W\overset{4}{-}WCl_4(dmpe)_2$ is also oxidized to $W_2Cl_6(dmpe)_2$ when dissolved in dichloromethane. With this reaction pathway, 1,3,5,7-$W_2Cl_6(dmpe)_2$ is produced in solution with no spectroscopic evidence for the complex 1,2,5,6-$W_2Cl_6(dmpe)_2$. However, as

---

(15) Morris, R. H. *Polyhedron* **1987**, *6*, 793.

(16) Klendworth, D. D.; Nimroy, T.; Salmon, D. J.; Walton, R. A.; Zeitlow, T. C. *Inorg. Chem.* **1981**, *20*, 947.

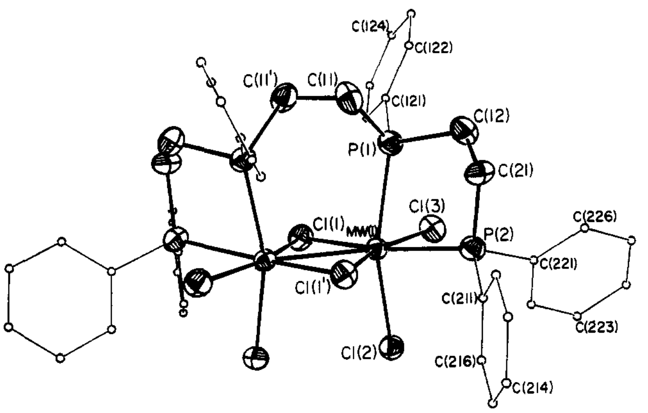

Figure 4. ORTEP drawing of 1,2,5,8-MoWCl$_6$(TETRAPHOS-1). Thermal ellipsoids for MW, P, and Cl are drawn at 50% probability, and the carbon atoms are represented by circles with fixed radii.

the dichloromethane is slowly evaporated, the compound 1,2,5,6-W$_2$Cl$_6$(dmpe)$_2$ is produced in the form of X-ray quality block-shaped crystals along with a small amount of uncharacterized brown oily residue. The ESBO ditungsten compounds may also be prepared by oxidative addition of Cl$_2$ to quadruply bonded complexes to form ESBO complexes. The reduction of WCl$_4$ with sodium triethylborohydride in THF to W(III) followed by the addition of the appropriate phosphine produces 1,3,5,7-W$_2$Cl$_6$(dmpe)$_2$ exclusively in low yield. Under these conditions no spectroscopic evidence for any other edge-sharing isomer was observed. Studies of the isomerization process have not been pursued to determine what factors such as time, solvent, or reaction conditions influence the process or whether it is reversible.

Structure and Bonding. The M$_2$X$_6$(L-L)$_2$ compounds reported here have been characterized by X-ray crystallography. The molecules possess geometries based on an edge-sharing bioctahedral arrangement of the core atoms. In complex **3**, the MM′Cl$_6$P$_4$ unit is arranged so that the equatorial plane is occupied by chelating phosphines and bridging chlorides and the four apical positions are filled by terminal chloride ligands. In the case of **1**, **2**, and **4**, the central MM′Cl$_6$P$_4$ core unit has essentially the same structure with two bridging chlorides, but the chelating polyphosphine occupies both equatorial and apical positions. The bond angles around the metal atoms form an octahedral arrangement distorted in the usual manner because of the presence of metal–metal bonding, viz., opening of the (μ-X)–M–(μ-X) angle and deviation from linearity of the angle Cl$_t$–M–Cl$_t$.[1]

The crystal structures of **2**–**4** show the type of disorder (i.e., random arrangement of the metal atoms) that is usually observed in heteronuclear systems. Therefore, the metal to ligand bond distances are averages of the Mo–L and W–L (L = Cl or P) distances due to the random arrangement of the M–M′ vector.[15] Because of this averaging, only the metal–metal bond lengths and overall conformations of **2**–**4** may be determined precisely.[11,17-19] The characteristics specific for each complex and the relationships between them will be explored in the following paragraphs.

Compounds 1 and 2. The ligand arrangement found in 1,2,5,6-W$_2$Cl$_6$(dmpe)$_2$ and 1,2,5,6-MoWCl$_6$(dmpe)$_2$ has not previously been reported for a M$_2$X$_6$(L-L)$_2$ type complex where the L-L unit is a bidentate phosphine ligand.[1] These two complexes are isostructural with only slight differences in molecular parameters. The metal–metal bond distances in **1** and **2** are indicative of a double bond. The W–W distance in **1**, 2.673(1) Å, is slightly shorter than the Mo–W distance in **2**, 2.695(1) Å, and the M–Cl$_b$–M angle is slightly more acute in **1** than in **2**. Both of these factors indicate that the metal–metal interaction in 1,2,5,6-W$_2$Cl$_6$(dmpe)$_2$ is slightly stronger than the interaction in 1,2,5,6-MoWCl$_6$(dmpe)$_2$, as expected and established in the literature. Complete bond distances and angles for 1,2,5,6-W$_2$Cl$_6$(dmpe)$_2$ are listed in Table IV, and a complete ORTEP drawing is given in Figure 2.

Compound 3. 1,3,5,7-MoWCl$_6$(dmpe)$_2$ represents the first example of a group VI ESBO complex with this structural type containing dmpe.[1,4] The structural characteristics are the same as 1,3,5,7-MoWCl$_6$(dppe)$_2$ with only subtle changes in bond lengths and angles. The most notable feature is a decrease in M–P distances and an increase in M–Cl$_b$ distances relative to 1,3,5,7-MoWCl$_6$(dppe)$_2$. This is, no doubt, a manifestation of the trans influence which has been observed in many other systems[20] including α-Mo$\overset{4}{-}$WCl$_4$(dmpe)$_2$. Complete bond distances and angles are listed in Table VIII, and a complete ORTEP drawing is shown in Figure 3.

A comparison of **2** with **3** reveals several changes in geometry and subtle changes in the molecular parameters. The geometric changes are obvious in the ORTEP drawings, shown in Figure 3. Neither phosphorus atom in **2** is in the equatorial plane; one is below and the other is above. This geometry does not result in a significant change in the M–M bond length (0.008 Å) but does result in significant changes in M–P and M–Cl distances. The changes in M–P and M–Cl distances reflect the nature of the atoms that are trans to the P or Cl. The M–P distances trans to Cl$_t$ in **2** are equal to the M–P distances trans to Cl$_b$, in **3**, but the M–P distances trans to Cl$_b$, in **2** are 0.03 Å longer than the other M–P distances in **3**. Both M–Cl$_b$ and M–Cl$_t$ distances are also ≈0.04 Å longer in **2** than in **3** due to the influence of the atoms trans to the atoms in question.[20] Complete bond distances and angles are listed in Table VI, and a complete ORTEP drawing is given in Figure 3.

Compound 4. 1,2,5,8-MoWCl$_6$(TETRAPHOS-1) is one of the more interesting complexes in this study, at least from a structural standpoint. Neither the Mo$_2$ nor the W$_2$ analog of this complex has been structurally characterized or is, in fact, even known. The nature of the TETRAPHOS-1 ligand is such that it has produced a new type of ligand distribution (1,2,5,8) for an ESBO complex. The tetradentate phosphine ligand arrangement consists of two chelating diphosphine units and one bridging diphosphine unit to produce an axis of 2-fold symmetry orthogonal to the metal–metal axis, and the molecule is chiral. It is interesting that **4** crystallizes in a chiral space group, *I*23, so that entire crystals are enantiomorphs, rather than having, as is far more common, pairs of enantiomorphic molecules packed to give nonchiral crystals.

The metal–metal bond distance in this complex is 2.718(2) Å. This separation is essentially an average of the metal–metal bond distances for 1,3,5,7-MoWCl$_6$(dppe)$_2$ and 2,4,6,8-MoWCl$_6$(μ-dppm)$_2$. One might consider the geometry of **4** to be halfway between the two (one bridging phosphine, and two P atoms in the equatorial plane). The M–P, M–Cl$_b$, and M–Cl$_t$ bond lengths are essentially equal to their counterparts in 1,3,5,7-MoWCl$_6$(dppe)$_2$ and 2,4,6,8-MoWCl$_6$(μ-dppm)$_2$, (i.e. M–P trans to Cl, M–Cl trans to P, and M–Cl trans to Cl).[21] There are some distortions in the bond angles caused by the polydentate phosphine ligand and these distortions cause the molecule to twist slightly with respect to the metal–metal vector. Table XI contains selected torsional angles. Selected bond distances and angles are listed in Table X, and a complete ORTEP drawing is shown in Figure 4.

Magnetic Behavior. The magnetic behavior of these molecules will be determined by the electronic states that are thermally accessible. Because of the very similar energies of the δ and δ^*

---

(17) Cotton, F. A.; Hanson, B. E. *Inorg. Chem.* **1978**, *17*, 3237.
(18) Katovic, V.; McCarley, R. E. *J. Am. Chem. Soc.* **1978**, *100*, 5586.
(19) Garner, C. D.; Senior, R. G.; King, T. J. *J. Am. Chem. Soc.* **1976**, *98*, 3526.
(20) Cotton, F. A.; Felthouse, T. R. *Inorg. Chem.* **1981**, *20*, 3880.
(21) Cotton, F. A.; Eglin, J. L.; James, C. A.; Luck, R. L. *Inorg. Chem.* **1992**, *31*, 5308.

Table XI. Selected Torsional Angles (deg) for 1,2,5,8-MoWCl$_6$(TETRAPHOS-1) (**4**)[a]

Cl(1)–MW(1)[b]–MW(1)′–P(2)′	−8.69(26)
Cl(2)–MW(1)–MW(1)′–Cl(2)′	−7.90(21)
Cl(3)–MW(1)–MW(1)′–Cl(1)	0.66(30)
Cl(3)–MW(1)–MW(1)′–P(2)′	−8.03(34)
P(1)–MW(1)–MW(1)′–P(1)′	−10.47(22)
P(2)–MW(1)–MW(1)′–Cl(1)′	−8.69(26)
P(2)–MW(1)–MW(1)′–Cl(3)′	−8.03(34)
Cl(1)′–MW(1)–MW(1)′–Cl(3)′	0.66(30)

[a] Numbers in parentheses are estimated standard deviations in the least significant digit. [b] Hybrid metal atom composed of 55.8 (16)% Mo and 44.2 (16)% W.

Table XII. Calculated Magnetic and Electronic Parameters for 1,2,5,6-W$_2$Cl$_6$(dmpe)$_2$ and 1,2,5,6-MoWCl$_6$(dmpe)$_2$

complex	$-2J$, cm^{-1}	A, MHz	H_{dia}, ppm
1,2,5,6-W$_2$(μ-Cl)$_2$Cl$_4$(dmpe)$_2$	−1006	P–W = 40.6 P–W = 51.8	P–W = 67.58 P–W = −94.5
1,3,5,7-W$_2$(μ-Cl)$_2$Cl$_4$(dmpe)$_2$	−1024	P–W = 31.2	P–W = 10.48

orbitals, several states must be considered.[22] Although the relative energies of the δ and δ^* orbitals are uncertain, the qualitative pattern of states to be considered is predictable.[22,23] The lowest and highest states will be $^1A_{1g}$, and between these states there are the $^3B_{1u}$ and $^1B_{1u}$ states. The temperature dependent magnetic behavior of these molecules is reflected in the temperature dependence of the $^{31}P\{^1H\}$ NMR chemical shifts. This dependence may in turn be used to establish the magnitude of the singlet–triplet gap using variable temperature $^{31}P\{^1H\}$ NMR chemical shift data and eq 1,[24–27] where $\gamma_{(N)}$ is the gyromagnetic ratio of

$$H_{\text{obs}} = H_{\text{dia}} + \frac{2g\beta H_{0(N)}A}{(\gamma_{(N)}/2\pi)kT}(3 + e^{2J/kT})^{-1} \tag{1}$$

the nucleus, $H_{0(N)}$ is the resonance frequency of the nucleus, g and β are the Landé splitting factor and Bohr magneton for an electron, A is the hyperfine coupling constant between the electron and the nucleus in question, H_{dia} is the resonance frequency of the nuclei in an equivalent diamagnetic environment, $-2J$ is the singlet–triplet gap in the molecule, and the other symbols have their usual meaning.

The $-2J$ values determined for **1** and **5** are based on the assumption that excited states of still higher energy than the triplet do not contribute significantly to the magnetic properties and that the metal-centered dipolar contributions to the paramagnetic shifts are not significant.[21] The calculated values of $-2J$, A, and H_{dia} for **1** and **5** are listed in Table XII.

The $-2J$ values determined agree quite well with the values reported in the literature for other homonuclear ditungsten ESBO complexes obtained from both bulk magnetic susceptibility measurements and variable temperature $^{31}P\{^1H\}$ NMR spectroscopy. While the $-2J$ values are not significantly different for the two isomers of this complex, there is a significant difference in the chemical shift values of the nonequivalent phosphorus atoms of 1,2,5,6-W$_2$Cl$_6$(dmpe)$_2$ which has also been observed in W$_2$Cl$_6$(PEt$_3$)$_4$.[7]

Metal–Metal Bonding. The question of how the d^3–d^3 configurations interact with one another is a major topic of interest in the study of Mo$_2^{6+}$ and W$_2^{6+}$ complexes.[4,6,22,23] The MoW^{6+} complexes are subject to the same constraints and considerations as the Mo$_2^{6+}$ and W$_2^{6+}$ complexes. The accurate determination of the singlet–triplet gaps for **1** and **5** indicate that the δ^* to δ or δ to δ^* separation is small. Therefore, these orbitals may be considered to be nonbonding in character and the bond order in these complexes is effectively 2. The double bond arises from the fact that the σ and π levels are each doubly occupied. This is the same conclusion previously reached for a series of Mo$_2$(μ-SR)$_2$Cl$_4$(L-L)$_2$ compounds based on both structural and theoretical data.[22]

Geometric Isomers of Edge-sharing Compounds. Edge-sharing bioctahedral complexes containing the M$_2$(μ-Y)$_2$X$_4$L$_4$ core, where X and Y are charged ligands and L is a neutral donor ligand, form only nine distinct geometric isomers, and these are shown in Figure 1. Of the nine isomers, examples of five have been previously reported in the literature for the M$_2$(μ-X)$_2$X$_4$P$_4$ core and two others are reported here for the first time. As the number and variety of these complexes has grown, we have perceived a need to develop a numbering scheme by which isomers may be distinguished. It should be noted that four of the isomers, ***5***, ***6***, ***8***, and ***9***, form enantiomers. Such a numbering system is shown in Figure 1. The equatorial ligands are assigned odd numbers (1, 3, 5, and 7) while the axial ligands are assigned even numbers (2, 4, 6, and 8). Note that the neutral ligands are numbered so that 1–4 are on one metal atom and 5–8 are on the other. In using this scheme, one of the neutral donor ligands in the equatorial plane should always be assigned number 1, and one of the neutral axial ligands cis to this position (if there is one) should be numbered 2. Further numbers should be chosen so as to use the lowest numbers possible. The use of this system gives rise to the unambiguous identification and easy recognition of the geometry from the compound name. In general, isomers having two adjacent axial positions occupied by P atoms [***1***, ***4***, ***5***, ***6***] would be expected only when the two P atoms are on the same ligand and connected by a CH$_2$ group.

A survey of the literature reveals a large number of ESBO complexes with the M$_2$(μ-Y)$_2$X$_4$L$_4$ core where L = neutral ligand.[1] However, in order to limit the scope of this discussion, our survey includes only compounds with the M$_2$(μ-X)$_2$X$_4$P$_4$ core where P = phosphine ligand. Of the 50 or so complexes that have been reported in the literature with a M$_2$(μ-X)$_2$X$_4$P$_4$ core, most belong to structural types ***1***, ***2***, or ***3***. These include variations where M = Zr, Hf, Nb, Ta, Cr, Mo, W, Re, Ru, and Rh; X = Cl, Br, or I; and P = PR$_3$, dppm, dppe, dmpe, or dmpm.

Examples of type ***1*** or 2,4,6,8 complexes generally contain bridging dppm or dmpm ligands and a variety of central metal atoms. Complexes reported in the literature include M = Nb,[28] Ta,[1] Cr,[29] Mo,[4] W,[4] Re,[4] Ru,[5] and Rh.[30]

Complex **3** is an example of a type ***2*** or 1,3,5,7 complex. Most of the reported 1,3,5,7 complexes are similar to this representative complex with only variations in the central metal atoms. Complexes of this type reported in the literature include M = Nb,[31] Ta,[32] Mo,[6] W,[6] and Re.[1] However, there are also complexes with monodentate phosphine ligands which possess this geometry. Complexes representative of this type include compounds where M = Zr[33] and Hf,[34] X = Cl and I, and P = PR$_3$.

The type ***3*** or 1,3,6,8 complex is the most common geometry

---

(22) Hopkins, M. D.; Gray, H. B.; Miskowski, V. M. *Polyhedron* **1987**, *6*, 705.

(23) Fisel, C. R.; Hoffmann, R.; Shaik, S.; Summerville, R. H. *J. Am. Chem. Soc.* **1980**, *102*, 4555.

(24) Campbell, G. C.; Haw, J. F. *Inorg. Chem.* **1988**, *27*, 3706.

(25) Campbell, G. C.; Reibenspies, J. H.; Haw, J. F. *Inorg. Chem.* **1991**, *30*, 171.

(26) Boersma, A. D.; Phillipi, M. A.; Goff, H. M. *J. Magn. Reson.* **1984**, *57*, 197.

(27) Holm, R. H.; Hawkins, C. J. In *NMR of Paramagnetic Molecules*; La Mar, G. N., Horrocks, W. D., Holm, R. H., Eds.; Academic Press: New York, 1973; Chapter 7.

(28) Cotton, F. A.; Duraj, S. A.; Falvello, L. R.; Roth, W. J. *Inorg. Chem.* **1985**, *24*, 4389.

(29) Cotton, F. A.; Eglin, J. L.; Luck, R. L.; Son, K. *Inorg. Chem.* **1990**, *29*, 1802.

(30) Cotton, F. A.; Dunbar, K. R.; Canich, J. M.; Falvello, L. R.; Price, A. C. *Inorg. Chem.* **1989**, *28*, 1754.

(31) Cotton, F. A.; Roth, W. J. *Inorg. Chem.* **1983**, *22*, 3654.

(32) Cotton, F. A.; Falvello, L. R.; Najjar, R. C. *Inorg. Chem.* **1983**, *22*, 375.

(33) Cotton, F. A.; Diebold, M. P.; Kibala, P. A. *Inorg. Chem.* **1988**, *27*, 799.

(34) Cotton, F. A.; Shang, M.; Wojtzak, W. A. *Inorg. Chem.* **1991**, *30*, 3670.

observed in ESBO complexes with four monodentate phosphines. This geometry has been reported for a variety of compounds with monodentate phosphines and many different metal atoms. This structural motif has been reported in compounds where M = Cr,[29] Mo,[35] W,[7] Re,[1] Ru,[36] and Rh.[30] However, no examples of heterobimetallic complexes of structural type *3* have been reported.

Examples of type *4* (1,2,7,8) and *5* (1,2,5,8) complexes are nonexistent in the literature, but one example of each has recently been synthesized and characterized. Both of these complexes utilize the steric demands of a polydentate phosphine ligand to obtain the unique geometries. The type *4* complex, 1,2,7,8-Mo_2Cl_6(eLTTP) (eLTTP = ethyl-substituted linear tetradentate phosphine),[37] is forced into this geometry by the meso nature (*S,S* or *R,R*) of the phosphine. The type *5* complex, 1,2,5,8-$MoWCl_6$(TETRAPHOS-1) is also forced into the unique geometry by the racemic nature (*R,S* or *S,R*) of the phosphine ligand.

Within the confines of a $M_2(\mu\text{-}X)_2X_4P_4$ core, there are no examples of complexes with the type *6* (1,2,6,7) geometry. However, if some variation in the bridging ligands is allowed, there are two reported examples of this structural motif. These are $Ta_2(\mu\text{-}O)(\mu\text{-}SMe_2)(dmpe)_2$ and $Ta_2(\mu\text{-}O)(\mu\text{-}THT)(py)_4$ [THT = tetrahydrothiophene].[38] The formation of the unique geometries in these cases is probably a balance between the trans influence of the bridging ligands and steric factors.

Complexes **1** and **2** are the only examples of type *7* (1,2,5,6) complexes with the $M_2(\mu\text{-}X)_2X_4P_4$ core. However, there is one other example, $Mo_2Cl_4(\mu\text{-}Cl)_2(DTO)_2$ [DTO = 3,6-dithiaoctane],[39] which has dithiolate ligands rather than diphosphine ligands. The occurence of this uncommon geometry is probably a result of the balance of the trans influence of the bridging ligands and steric factors.

We are unaware of any examples of type *8* (1,2,5,7) or *9* (1,2,6,8) complexes.

Electronic and Infrared Spectra. In the visible region of their electronic spectra, all the ESBO complexes display a prominent absorption band between 450 and 550 nm.[8,40] The exact origin of this absorption is unknown but comparisons in the series indicate that the position of this band is dependent on the nature of the metal center. All of the complexes also display strong ligand-to-metal charge-transfer bands below 400 nm.

$^{31}P\{^1H\}$ NMR Analysis. The homonuclear compounds 1,2,5,6-$W_2Cl_6(dmpe)_2$ and 1,3,5,7-$W_2Cl_6(dmpe)_2$ can be distinguished from one another by their distinct $^{31}P\{^1H\}$ NMR spectra. At sufficiently low temperatures, −80 °C, **1** exhibits two triplets of equal integrated intensity due to coupling between inequivalent phosphorus atoms, and **5** is a singlet, δ 1.52 ppm at −80 °C, with four equivalent phosphorus atoms.

In both 1,2,5,6-$W_2Cl_6(dmpe)_2$ and $W_2Cl_6(PEt_3)_4$, there are two sets of inequivalent phosphorus atoms. 1,2,5,6-$W_2Cl_6(dmpe)_2$ has two inequivalent phosphorus atoms on each end of the molecule and the two ends of the molecule are equivalent. The phosphorus atoms are coupled to one another (J = 97 Hz) to produce two triplets, one at δ 55.62 ppm and the other at δ −111.29 ppm at −90 °C. For $W_2Cl_6(PEt_3)_4$, one end of the molecule has two PEt_3 ligands in the axial positions and the other has two PEt_3 ligands in apical positions. These two sets of phosphorus atoms are coupled to one another (J = 87 Hz) to produce two triplets, one at δ 23.2 ppm and the other at δ −81.4 ppm at −80 °C.[7]

A firm assignment of chemical shifts has not been made for either compound. However, a tentative assignment can be made based on $^{31}P\{^1H\}$ NMR data obtained for the edge-sharing bioctahedral complex, $Rh_2Cl_6(PEt_3)_4$. The geometry of the dirhodium complex is analogous to $W_2Cl_6(PEt_3)_4$ and has two sets of inequivalent phosphorus environments. The downfield chemical shift with J_{Rh-P} = 111 Hz is due to the phosphorus ligands trans to a bridging chloride, and the upfield shift with J_{Rh-P} = 79 Hz, to the phosphorus ligands trans to another phosphorus atom.[41] By analogy, the downfield and upfield shifts in the spectrum of $W_2Cl_6(PEt_3)_4$ (δ 23.3 ppm and δ −81.4 ppm) might be similarly assigned. One might also tentatively assign the downfield shift (δ 55.62 ppm) in 1,2,5,6-$W_2Cl_6(dmpe)_2$ to the equatorial phosphorus ligands trans to bridging chlorides and the upfield shift (δ −111.29 ppm) to axial phosphorus ligands trans to axial chlorides.

Acknowledgment. We are grateful to Dr. Larry Falvello for assistance in X-ray crystallography and to the National Science Foundation for support.

Supplementary Material Available: Full lists of crystallographic data, torsional angles, bond distances, bond angles, anisotropic thermal parameters, and H atom positions (13 pages). Ordering information is given on any current masthead page.

---

(35) Mui, H. D.; Poli, R. *Inorg. Chem.* **1989**, *28*, 3609.
(36) Cotton, F. A.; Matusz, M.; Torralba, R. C. *Inorg. Chem.* **1989**, *28*, 1516.
(37) Cotton, F. A.; Hong, B. Unpublished results.
(38) Cotton, F. A.; Diebold, M. P.; Roth, W. J. *Inorg. Chim. Acta* **1988**, *149*, 105.
(39) Cotton, F. A.; Fanwick, P. E.; Fitch, J. W. *Inorg. Chem.* **1978**, *17*, 3254.
(40) Cotton, F. A.; Extine, M.; Gage, L. D. *Inorg. Chem.* **1978**, *17*, 172.
(41) Cotton, F. A.; Eglin, J. L.; Kang, S. *J. Am. Chem. Soc.* **1992**, *114*, 4015.